Research article

Crystallization behavior and structural evaluation of cordierite base glass-ceramic in the presence of CaO and B_2O_3 additives
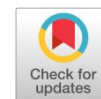
Zahra Shamohammadi Ghahsareh [ID], Mohammad Rezvani [ID] *

Department of Materials Engineering, University of Tabriz, Tabriz, Iran

A B S T R A C T

The purpose of the present work is to highlight the role of CaO and B_2O_3 additives on the crystallization behavior and microstructural properties of stoichiometric cordierite glass-ceramics using differential thermal analysis (DTA), X-ray diffraction (XRD), Fourier transform infrared spectroscopy (FTIR), Vickers micro-hardness and scanning electron microscopy (SEM). The results show that the presence of B_2O_3 and CaO in the initial glass led to the precipitation of only one exothermic peak (α-cordierite: $Mg_2Al_4Si_5O_{18}$). During the heat treatment process, the presence of calcium oxide favors crystallization of anorthite ($CaAl_2Si_2O_8$) besides α-cordierite phase. It is worth mentioning that, CaO and B_2O_3 additives strongly encourage the formation of α-cordierite and have the opposite effect on the crystallization of μ-cordierite. In order to determine the effect of crystallization and B_2O_3 and CaO additives on the hardness of specimens, the micro-hardness measurement of glasses and glass-ceramics shows that the glass-ceramic containing CaO (MAS5C) exhibits the highest micro-hardness value, which depends on the high crystallinity value in this specimen.

© 2022 The Authors. Published by Synsint Research Group.

1. Introduction

Cordierite glass-ceramics in the MAS system ($MgO–Al_2O_3–SiO_2$) have some valuable properties, including thermo-mechanical, chemical, and dielectric properties, which have received much attention during the past decades. These materials have a wide range of applications from cookware, glazes for floor tiles, kiln furniture, and heat exchangers to substrates in the microelectronic application and radomes [1–3]. Moreover, cordierite-based glass-ceramics are attractive materials due to their desirable mechanical properties (modulus (150 GPa) and strength (250 MPa)), low coefficient of thermal expansion, high thermal and chemical stability, and low dielectric constant (5.0 at 1 MHz). These features made these materials to be used as a substrate in low firing temperature substrates. These materials are also conventionally utilized in the electronic industry [4–8]. The synthesis of cordierite glass-ceramics is carried out by several methods (sol–gel,

solid-state reaction, and crystallization from glass) [9–11]. There are three polymorphic forms of magnesium cordierite ($Mg_2Al_4Si_5O_{18}$): metastable phase (solid solution with a β-quartz structure) called μ-cordierite, β-cordierite phase (low-temperature orthorhombic), and indialite or α-cordierite (high-temperature hexagonal) [6, 12, 13].

Comprehensive research on the crystallization behavior, kinetics, thermal and mechanical properties of cordierite glass-ceramics has been conducted and is still ongoing [3, 4, 8, 12–14]. Glass-ceramics are prepared by heat treatment of the suitable composition of glasses. Cordierite glass-ceramics with the major crystalline phase of the α-cordierite can be obtained by heating the glasses in the temperature range of 900 to 1200 °C. The effects of various additives, chemical composition, and heat treatment process on crystallization mechanisms, structural, mechanical and thermal properties of these glass-ceramics have been studied in some literature [2, 3, 7, 14–20]. The effects of nucleating and fluxing agents (e.g., TiO_2, CeO_2, V_2O_5, CrO_3, NiO,

---

B_2O_3, and alkaline oxides) on the crystallization mechanisms of cordierite glasses have been examined in some studies [6–14, 20, 21]. In fact, in the glass specimens, small amounts of additives in the composition of glass specimens can significantly influence the viscosity and crystallization behavior of the glass-ceramics [14].

Yu et al. [22] have investigated the synthesis of cordierite phase from perlite (as raw material) for low temperature co-fired application. In this case, α-cordierite glass-ceramics were fabricated by low-temperature heat treatment (900–950 °C), which resulted in dielectric constants and thermal expansion coefficients 5.6–6.1 and 2.56–2.91×10^{-6} K^{-1}, respectively. Maeda et al. [23] have examined the effect of molybdenum on the MAS system and showed that in the application of high thermal endurance, MoO_3 can be the superior nucleating agent in this system. Kang et al. [24] have reported the effect of Na_2O, Li_2O, and K_2O on the acid corrosion resistance of cordierite glass-ceramics. Adding 1.5 mol% Na_2O as well as 1.5 mol% Li_2O to the primary glass specimen heat treated at 880 °C has exhibited the optimal acid resistance. The minimum weight loss of this glass-ceramic specimen has been about 0.096%. Yu et al. [25] have reported that the crystallization mechanism of the glass specimen containing $TiO_2+ZrO_2+P_2O_5$ demonstrates a tendency to bulk crystallization. In this case, $TiO_2+ZrO_2+P_2O_5$ act as the nucleating agent in this system. Considering the obtained results, the thermal expansion coefficient and micro-hardness have been reported as 1.4×10^{-6} °C^{-1} (at 20–300 °C) and 7.4 GPa, respectively. Lao and Xu [26] have studied the effect of talc, Al_2O_3 content, and MgO/SiO_2 ratio on the crystallization behavior of non-stoichiometric cordierite specimens. It has been found that in the presence of 15 wt% talc as well as increasing the M/S ratio, the crystallization peak temperature of the specimen decreased from 1085 °C to 1052.2 °C. The specimen containing the lowest amount of Al_2O_3 along with 15 wt% talc has shown the lowest porosity (0.3%) among the studied specimens.

To our knowledge, there is no sufficient study on the effect of CaO and B_2O_3 additives on cordierite glass and glass-ceramic formed by melting method (using analytical grade reagents of SiO_2, Al_2O_3, and MgO). In this work, cordierite glass-ceramics were prepared using homogenous glasses by crystal growth method. This study aims to highlight the role of CaO and B_2O_3 additives on the glass properties and the crystallization behavior of stoichiometric cordierite composition. In this regard, the production of glass-ceramic with the highest amount of crystallinity, taking into account the precipitation of the α-cordierite phase to obtain improved properties including micro-hardness and microstructural characteristics has been considered.

2. Experimental procedures

Stoichiometric cordierite composition including 51.8 SiO_2, 34.8 Al_2O_3, and 13.4 MgO (wt%) was utilized as the base composition. The raw materials were analytical grade reagents of $MgCO_3$, Al_2O_3, SiO_2, $CaCO_3$, and B_2O_3. The stoichiometric cordierite composition was used as a base and named MAS. The specimens MAS1B and MAS5C were prepared by adding 1 and 5 wt% ratios of B_2O_3 and CaO to the stoichiometric composition, respectively. The MAS1B5C composition was made by adding both B_2O_3 and CaO additives to the base specimen (MAS). Table 1 shows the chemical compositions of studied glasses in the presence of CaO and B_2O_3 additives. The obtained powder mixtures were melted in zircon crucibles at 1600 °C for 2 h using an electric furnace. Afterward, the molten specimens were poured

Table 1. Chemical composition of glass specimens (wt% ratios).

Specimen/oxide	SiO$_2$	Al$_2$O$_3$	MgO	B$_2$O$_3$	CaO
MAS	51.8	34.8	13.4	-	-
MAS1B	51.8	34.8	13.4	1	-
MAS5C	51.8	34.8	13.4	-	5
MAS1B5C	51.8	34.8	13.4	1	5

into the stainless-steel molds and annealed in a muffle furnace at 600 °C for 1 h.

To investigate the crystallization behavior of resulting glass powders, a differential thermal analyzer (DTA) (Shimadzu DTG 60 AH) was used at the heating rate of 10 °C min^{-1}. The curves of DTA were recorded at 20–1200 °C using 50 mg of each glass powder. The reference material for each DTA run was α-Al$_2$O$_3$ powder. The X-ray diffractometer (Siemens-D500, 30 mA, 40 kV, and Cu K$_\alpha$ radiation) was used to prove the amorphous inherence of the as-prepared glasses as well as identify the crystalline phases precipitated during the heat treatment process. High Score Plus software was used to analyze the spectra in the range of 10–70 ° 2θ. The structural features of glass specimens were analyzed by Fourier transform infrared spectrophotometer (FT-IR, Tensor 27 Bruker Company) at room temperature and using the KBr-pellet technique. Five scans were taken for each spectrum in the range of 400–1400 cm^{-1}. A scanning electron microscope (Mira3 Feg-SEM Tescan) was used to evaluate the microstructural characteristics of cordierite glass-ceramics. The glass-ceramic specimens were polished and etched with 5 vol% HF solution for 90 s (20 °C), then washed with distilled water and dried. Finally, the specimens were coated using a thin layer of gold. The Vickers micro-hardness (Zwick/Roell ZHV10
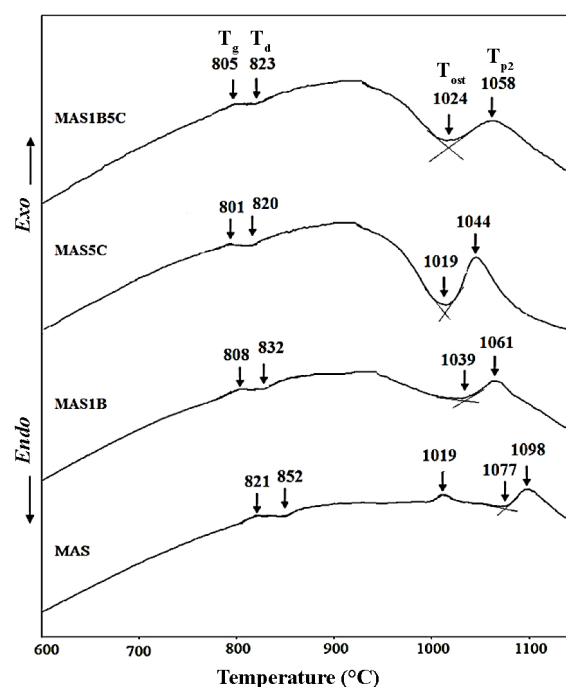

Fig. 1. DTA curves of glass specimens in the presence of CaO and B_2O_3 additives at the heating rate of 10 °C min^{-1}.
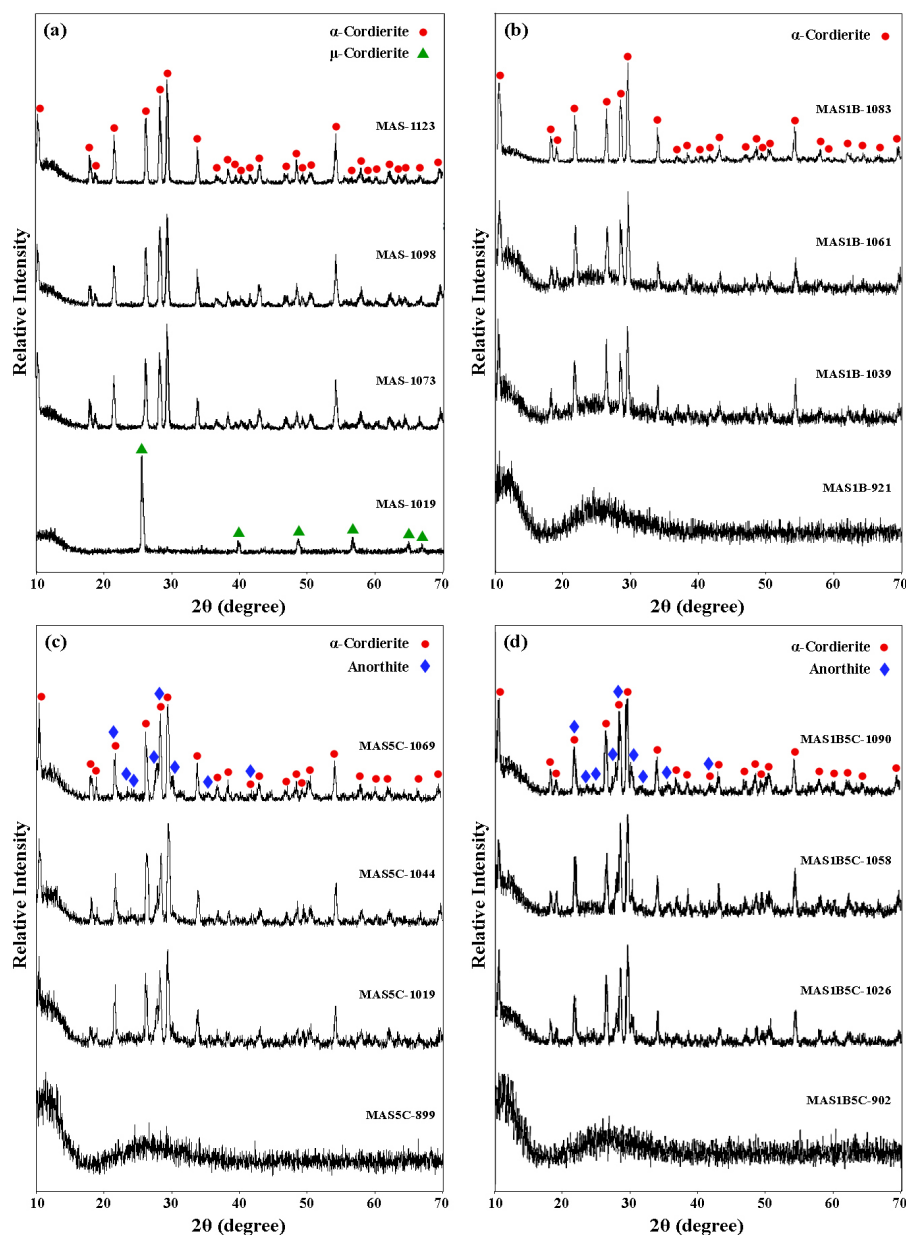
Fig. 2. XRD patterns of a) MAS, b) MAS1B, c) MAS5C, and d) MAS1B5C glasses heat treated at different temperatures.

micro-hardness) was carried out using the indentation method. Polished glass and glass-ceramic specimens were used for indentation. The mean value of the results was reported for each specimen. The applied load during the hardness measurement (diamond indenter) was 200 g for 15 s.

3. Results and discussion

3.1. Crystallization behavior and crystalline phase evolution

In order to investigate the thermal behaviors of the glass powders, DTA curves were utilized. Considering Fig. 1, these curves include the crystallization peak (T_P) and the glass transition (T_g) temperatures. The MAS specimen exhibited two exothermic peaks at 1019 and 1098 °C that can be attributed to the crystallization of μ- and α-cordierite,

respectively. In fact, μ-cordierite precipitated at a lower temperature, and by a gradual increase in temperature, the crystalline phase transformed from μ-cordierite to α-cordierite. However, in specimens containing CaO and B_2O_3, only one exothermic peak appeared between 1040–1065 °C that can be attributed to the α-cordierite. According to the DTA curves, in the presence of CaO and B_2O_3 additives, the initial glass composition deviated from the stoichiometric state. As a result, the tendency to crystallization of the μ-cordierite decreased, and α-cordierite crystallized as a single phase at lower crystallization peak temperatures.

According to Fig. 1, the crystallization peak temperature of the MAS5C specimen is sharper than other specimens, and it is obvious that this temperature has decreased by about 54 °C compared to the base specimen. As we know, Ca^{2+} ion is a modifier cation in the glass (a large cation with a small charge). This ion can disrupt the silicate

network and also weaken the structure of the glass network by increasing the number of non-bridging oxygen ions (NBO) [9, 27, 28]. As shown in Fig. 1, the glass transition and crystallization peak temperatures of the MAS5C specimen have decreased. As it is evident from Fig. 1, the MAS1B glass specimen has slightly higher crystallization peak and glass transition temperatures compared to the MAS5C glass specimen, representing the higher viscosity of the mentioned glass. In this case, the tendency to crystallize has decreased due to the role of the B_2O_3 additive as a network former in the structure [29–31]. It has also been reported that this behavior is attributed to the glass-forming ability of B_2O_3. In this way, the glass network connectivity of the specimen can be improved by reducing the non-bridging oxygens in the glass structure [14, 27]. The presence of μ- and α-cordierite phases and small amounts of the anorthite phase (in CaO containing glasses) can be shown by X-ray analysis (Fig. 2).

Fig. 2 illustrates the XRD patterns of all crystallized specimens at different temperatures (e.g., the crystallization peak temperature) obtained by DTA curves. Fig. 2a shows the XRD patterns of the MAS glass. According to HighScore Plus software, the diffraction peak at $2\theta=25.712$ ° depends on the μ-cordierite phase (00-027-0716). As shown in Fig. 2a, by the gradual increase of temperature from T_{p1} (μ-) to T_{p2}, the μ-cordierite phase has disappeared from the pattern and α-cordierite phase (00-002-0646) precipitated ($2\theta=25.712$ ° (μ-cordierite) to $2\theta=26.408$ ° (α-cordierite)).

From the XRD data (Fig. 2), it is found that the precipitation of μ-cordierite is not detected in the glass-ceramics containing CaO and B_2O_3 additives. In these specimens, only α -cordierite was exhibited as the main crystalline phase. As seen in Figs. 2c & 2d, the peak of the anorthite phase (00-041-1486) can also be detected as a secondary crystalline phase in CaO containing glasses. In general, in the MgO–Al_2O_3–SiO_2 glass system, μ-cordierite is crystallized at a lower temperature during the heat treatment process, and with increasing temperature, this phase is transformed into α-cordierite at about 1050 °C. The mechanical properties of α-cordierite are better than μ-cordierite [2, 8, 12–14, 19].

Considering the positive effect of α-cordierite, the glasses containing CaO and B_2O_3 additives, which showed only the α-cordierite phase as the main crystalline phase at low temperatures, are more suitable specimens than the stoichiometry specimen. According to previous reports, CaO can intensify the precipitation of α-cordierite and simultaneously suppresses the precipitation of μ-cordierite in the MgO–Al_2O_3–SiO_2 system [9, 14, 21]. Also, Ca^{2+} and B^{3+} ions have the most significant effect in decreasing the melting temperature of MAS specimens [9, 27]. In fact, the effect of Ca^{2+} ions on the structure of the glass network is due to the weak bonding of Ca–O compared to Mg–O (the field strength of Ca^{2+} cations is lower than Mg^{2+} cations), which leads to an increase in the mobility of the elements in the glass network [20].

Ohlberg and Strickler method (Eq. 1) was utilized for the quantitative measurement of crystallinity in all specimens [32].

$$V_t = \frac{100(I_g - I_x)}{I_g - I_b} \qquad (1)$$

Where V_t, I_g, I_x, and I_b refer to the volume fraction of crystallization, the X-ray scattering intensity of primary glass, crystallized glass, and the mechanical mixture of oxide powders, respectively. A modified version of the above method suggests using some 2θ values instead of a single 2θ value. At three 2θ values of 52, 32, and 17 ° for each glass-ceramic specimen, the average crystallinity content is summarized in Table 2. In MAS, MAS1B, and MAS5C glasses, the higher the temperature, the higher the crystallization. However, in MAS1B5C glass, the crystallinity value of the sample decreased with increasing temperature. This may be attributed to the simultaneous presence of
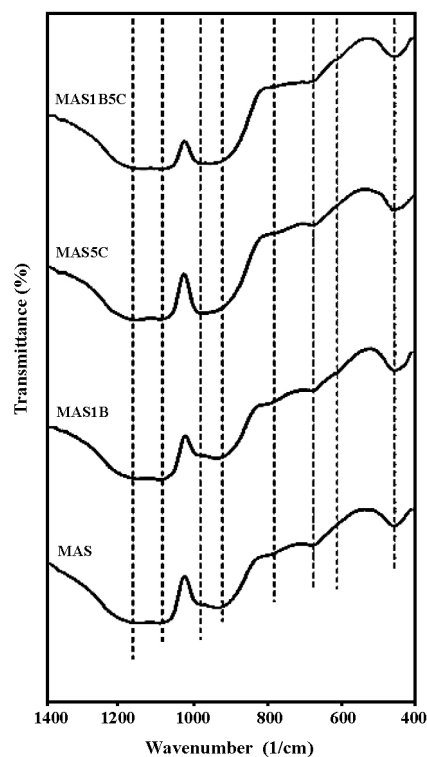
Table 2. Crystallization values of specimens at different heat treatment temperatures.

Specimen	Heat treatment temperature (°C)	V_t
MAS	1019	22±4
	1073	49±2
	1098	57±8
	1123	59±3
MAS1B	1039	27±1
	1061	35±3
	1083	42±5
MAS5C	1019	46±2
	1044	67±6
	1069	75±3
MAS1B5C	1026	32±4
	1058	65±6
	1090	57±9

Fig. 3. FTIR spectroscopy of the initial glasses in the presence of CaO and B_2O_3.

both additives in the glass network (CaO and B_2O_3 additives). The presence of a secondary phase (anorthite) and the network former ability of B_2O_3 have reduced the crystallinity of the MAS1B5C specimen. In fact, cordierite and anorthite have similar elements in their composition. For this reason, the crystallization of anorthite can reduce some of the essential elements that are necessary for the precipitation of cordierite. In these conditions, with the gradual increase in temperature, the total crystallinity of the MAS1B5C specimen has decreased.

It is obvious that the MAS5C-1069 glass-ceramic specimen exhibited the highest crystallinity among all specimens. As we know, CaO as a network modifier enhances the number of non-bridging oxygen (NBO) in the glass structure, which leads to lower viscosity, as well as lower glass transition and crystallization peak temperatures. These changes have improved the crystallinity in this specimen [9, 27, 28]. MAS1B-1061 specimen showed the lowest crystallinity among heat treated specimens at the second crystallization peak temperature. Considering the role of B_2O_3 as a network former in the glass, the specimen containing B_2O_3 had lower crystallinity among all specimens [14, 27].

To determine the role of Ca^{2+} and B^{3+} ions in the glass structure,

Fig. 5. SEM micrograph of the heat-treated MAS1B glass at 70,000 magnification.

Fourier Transform Infrared Spectroscopy was utilized. This analysis is used to evaluate vibrations caused by stretching and bending movements of atoms in a molecule. In fact, the bonds that make up the molecules are examined. FTIR spectra of the glass specimens are given in Fig. 3. In most cases, light irradiation from 1400 to 400 cm^{-1} (the mid-infrared) is utilized for inorganic compounds [33]. Considering Fig. 3, three main bonds (1200–1050, 800–650, 500–400 cm^{-1}) can be recognized in the spectra of the glass specimens related to silicon bonds [34–37]. Asymmetric stretching vibrations, symmetric stretching

Fig. 4. SEM micrographs of the heat-treated MAS glass at a) 40,000 and b) 70,000 magnifications.

Table 3. Vickers micro-hardness for glass and glass-ceramic specimens.

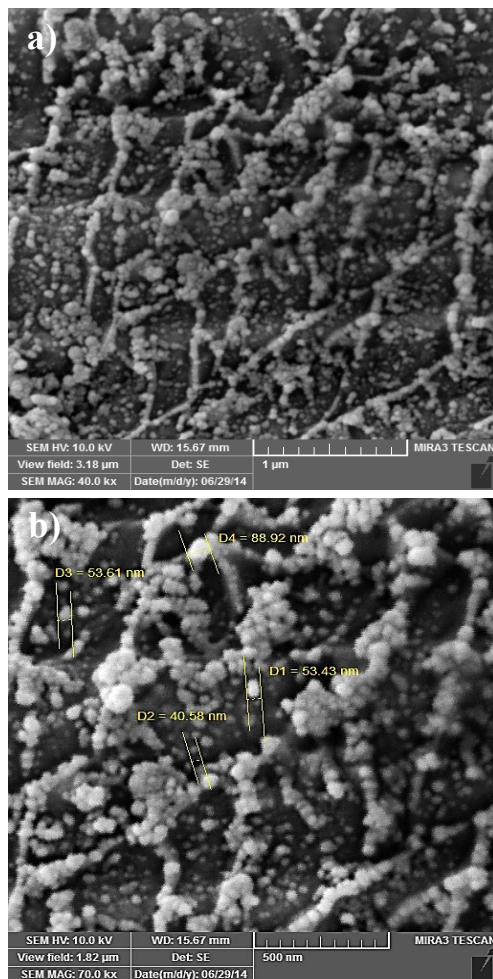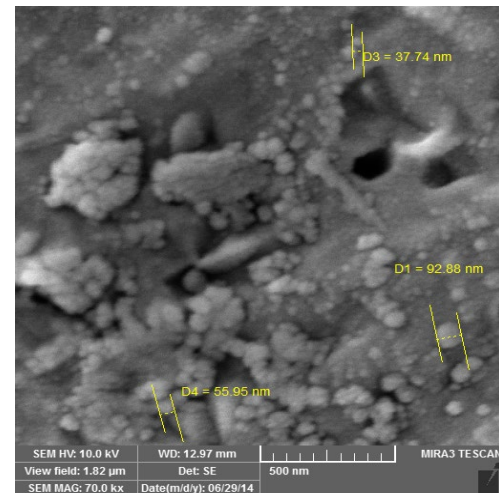| Specimen	Heat treatment temperature (°C)	Vickers micro-hardness (GPa)
MAS	-	7.56 (± 0.75)
	1019	9.35 (± 0.77)
	1073	10.25 (± 0.63)
	1098	10.70 (± 0.84)
	1123	11.20 (± 0.89)
MAS1B	-	7.45 (± 0.67)
	1039	-
	1061	10.23 (± 0.90)
	1083	10.37 (± 0.68)
MAS5C	-	7.40 (± 0.81)
	1019	10.42 (± 0.80)
	1044	11.23 (± 0.71)
	1069	11.84 (± 0.68)
MAS1B5C	-	7.52 (± 0.73)
	1026	10.29 (± 0.93)
	1058	11.10 (± 0.69)
	1090	10.77 (± 0.66)

Fig. 6. SEM micrographs of the heat-treated MAS5C glass at a) 40,000 and b) 70,000 magnifications.
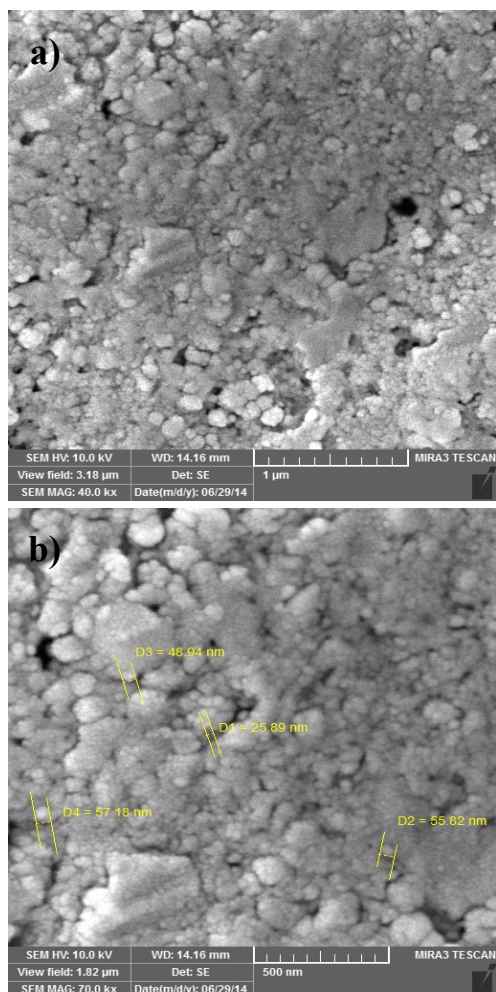

Fig. 7. SEM micrographs of the heat-treated MAS1B5C glass at a) 40,000 and b) 70,000 magnifications.

vibrations, and bending vibrations of the Si–O–Si bond of SiO_4 tetrahedral can be observed at about 1080 cm^{-1} (besides a mild shoulder at 1200 cm^{-1}), 669 cm^{-1} (besides 781 cm^{-1}), and 459 cm^{-1}, respectively.

As we know, in the presence of Al_2O_3, Al^{3+} ions can replace Si^{4+} ions in the SiO_4 tetrahedral and form AlO_4 tetrahedral. In these cases, an absorption bond corresponding to the asymmetric stretching vibration of Si–O–Al is figured out at about 931 cm^{-1} besides a shoulder at 994 cm^{-1} [38, 39]. In CaO containing glasses, there is another peak at about 994 cm^{-1} corresponding to the Si–O–Ca bond, which overlaps with the Si–O–Al vibrational mode [40]. For this reason, in MAS5C and MAS1B5C glasses, the Si–O–Ca bond, along with the Si–O–Al asymmetric stretching vibration bond, has caused a sharper peak at 994 cm^{-1}. In the glass containing B_2O_3, there is a weak peak at 604 cm^{-1} related to the B–O–Si bending vibration mode [41].

3.2. Vickers micro-hardness

The Vickers micro-hardness results of the glass and glass-ceramic specimens are given in Table 3. According to Table 3, the hardness values of the glass-ceramic specimens are much higher than those of glass specimens, ranging from 7.40 to 11.84 (GPa) for glass and glass-ceramic, respectively. It is known that glass-ceramic specimens
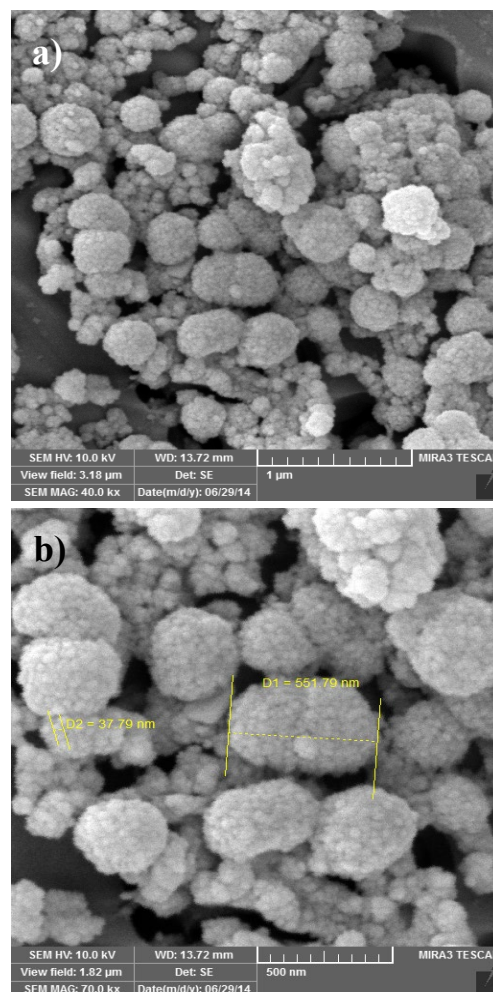
demonstrate a higher hardness compared to glassy systems because the crystalline phases are usually harder than glassy phases. Among the studied specimens, MAS5C glass-ceramic heat treated at 1069 °C showed the highest hardness value corresponding to higher crystallinity in this specimen.

According to Table 2, the MAS1B glass-ceramic heat treated at 1039 °C had the lowest crystallinity among other MAS1B specimens. Considering the role of B_2O_3 as a network former in the MAS system, the crystallization mechanism of B_2O_3 containing glass-ceramics was surface crystallization. As a result, glass-ceramic-1039 had a low level of surface crystallinity which was removed by polishing, leaving a glassy phase below the polished region (center of the specimen). For this reason, this specimen failed and could not be used for the hardness test. However, glass-ceramics containing B_2O_3 had the lowest hardness among all glass-ceramics.

3.3. Microstructural investigation

SEM micrographs of glass-ceramic specimens after heat treatment at the crystallization peak temperatures have been shown in Figs. 4–7. SEM micrographs of the specimens show complete crystallization on the surface. It can also be illustrated that the obtained crystals

(α-cordierite) are uniformly dispersed in the glass matrix in terms of size and shape. According to the DTA curves shown in Fig. 1, it can be seen that the crystallization peak temperature of the MAS5C specimen is much sharper than other specimens. This is evidence of a higher crystallization rate in this specimen. In the MAS5C glass, it seems that the low viscosity of the glass has assisted the crystallization process. The average crystal size was 40 nm and the maximum crystal size was about 90 nm, which are homogeneously distributed among the glass matrix.

4. Conclusions

In this study, the crystallization behavior of cordierite glass-ceramics in the MgO–Al$_2$O$_3$–SiO$_2$ system containing CaO and B$_2$O$_3$ additives was studied. According to the DTA curves, the MAS specimen exhibited two exothermic peaks, which can be attributed to the crystallization of μ- and α-cordierite, respectively. However, in other specimens, only one exothermic peak (for the formation of α-cordierite) appeared. For both heat-treated glasses containing CaO, the anorthite phase was precipitated as a secondary crystalline phase. With the gradual increase in temperature, the intensity of anorthite peaks in XRD patterns has also increased. Considering the DTA curves, the crystallization peak temperature of the MAS5C specimen was lower than the other specimen. In fact, the MAS5C glass-ceramic had a lower viscosity due to the role of CaO as a network modifier in the glass structure. Among the studied specimens, the MAS5C specimen exhibited the highest micro-hardness value, which depends on the high crystallinity value in this specimen. In contrast, B$_2$O$_3$ containing glass-ceramic had a lower micro-hardness value due to lower crystallinity value in this specimen, which is related to the role of B$_2$O$_3$ as a network former in the structure.

CRediT authorship contribution statement

Zahra Shamohammadi Ghahsareh: Investigation, Resources, Software, Data curation, Formal Analysis, Writing – original draft.
Mohammad Rezvani: Project administration, Supervision, Validation, Writing – review & editing.

Data availability

The data underlying this article will be shared on reasonable request to the corresponding author.

Declaration of competing interest

The authors declare no competing interests.

Funding and acknowledgment

References

[1] G.-h. Chen, X.-y. Liu, Influence of AlN addition on thermal and mechanical properties of cordierite-based glass/ceramic composites, J. Mater. Process. Technol. 190 (2007) 77–80. https://doi.org/10.1016/j.jmatprotec.2007.03.106.

[2] V. Marghussian, U. Balazadegan, B. Eftekhari-yekta, The effect of BaO and Al2O3 addition on the crystallization behaviour of cordierite glass-ceramics in the presence of V2O5 nucleant, J. Eur. Ceram. Soc. 29 (2009) 39–46. https://doi.org/10.1016/j.jeurceramsoc.2008.05.026.

[3] V.K. Marghussian, O. Balazadegan, B. Eftekhari-yekta, Crystallization behaviour, microstructure and mechanical properties of cordierite–mullite glass-ceramics, J. Alloys Compd. 484 (2009) 902–906. https://doi.org/10.1016/j.jallcom.2009.05.080.

[4] H. Shao, K. Liang, F. Peng, Crystallization kinetics of MgO–Al2O3–SiO2 glass-ceramics, Ceram. Int. 30 (2004) 927–930. https://doi.org/10.1016/j.ceramint.2003.10.015.

[5] N.J. Azin, M.A. Camerucci, A.L. Cavalieri, Crystallization of non-stoichiometric cordierite glasses, Ceram. Int. 31 (2005) 189–195. https://doi.org/10.1016/j.ceramint.2004.04.002.

[6] M.A. Villegasa, J. Alarcón, Mechanism of crystallization of Co-cordierites from stoichiometric powdered glasses, J. Eur. Ceram. Soc. 22 (2002) 487–494. https://doi.org/10.1016/S0955-2219(01)00300-4.

[7] M. Terada, K. Kawamura, I. Kagomiya, K. Kakimoto, H. Ohsato, Effect of Ni substitution on the microwave dielectric properties of cordierite, J. Eur. Ceram. Soc. 27 (2007) 3045–3048. https://doi.org/10.1016/j.jeurceramsoc.2006.11.050.

[8] G.-H. Chen, X.-Y. Liu, Sintering, Crystallization and properties of MgO–Al2O3–SiO2 system glass-ceramics containing ZnO, J. Alloys Compd. 431 (2007) 282–286. https://doi.org/10.1016/j.jallcom.2006.05.060.

[9] H. Malekzadeh, M. Rezvani, Effect of CaO additive on sintering and crystallization behavior of cordierite glass-ceramic prepared by sol-gel method, J. Sol-Gel Sci. Technol. 66 (2013) 199–205. https://doi.org/10.1007/s10971-013-2992-y.

[10] R. Goren, H. Gocmez, C. Ozgur, Synthesis of cordierite powder from talc, diatomite and alumina, Ceram. Int. 32 (2006) 407–409. https://doi.org/10.1016/j.ceramint.2005.03.016.

[11] M.J. Maleki, H. Majidian, S. Banijamali, M. Zakeri, Development of cordierite-based glass-ceramics by slip casting through selecting the appropriate sintering conditions, Synth. Sinter. 2 (2022) 84–91. https://doi.org/10.53063/synsint.2022.22116.

[12] S. Wang, K. Liang, Crystallization behavior and infrared radiation property of nickel–magnesium cordierite based glass–ceramics, J. Non-Cryst. Solids. 354 (2008) 1522–1525. https://doi.org/10.1016/j.jnoncrysol.2007.08.031.

[13] S. Wang, F. Kuang, Q. Yan, Ch. Ge, L. Qi, Crystallization and infrared radiation properties of iron ion doped cordierite glass-ceramics, J. Alloys Compd. 509 (2011) 2819–2823. https://doi.org/10.1016/j.jallcom.2010.11.126.

[14] Y. Demirci, E. Günay, Crystallization behavior and properties of cordierite glass-ceramics with added boron oxide, J. Ceram. Process. Res. 12 (2011) 352–356.

[15] M. Dittmer, M. Müller, C. Rüssel, Self-organized nano crystallinity in MgO–Al2O3–SiO2 glasses with ZrO2 as nucleating agent, Mater. Chem. Phys. 124 (2010) 1083–1088. https://doi.org/10.1016/j.matchemphys.2010.08.037.

[16] J. Banjuraizah, H. Mohamad, Z.A. Ahmad, Crystal structure of single phase and low sintering temperature of α-cordierite synthesized from talc and kaolin, J. Alloys Compd. 482 (2009) 429–436. https://doi.org/10.1016/j.jallcom.2009.04.044.

[17] S.K. Marikkannan, E.P. Ayyasamy, Synthesis, characterization and sintering behavior influencing the mechanical, thermal and physical properties of cordierite-doped TiO2, J. Mater. Res. Technol. 2 (2013) 269–275. https://doi.org/10.1016/j.jmrt.2013.03.016.

[18] B.J. Banjuraizah, H. Mohamad, Z.A. Ahmad, Thermal expansion coefficient and dielectric properties of non-stoichiometric cordierite compositions with excess MgO mole ratio synthesized from mainly kaolin and talc by the glass crystallization method, J. Alloys Compd. 494 (2010) 256–260. https://doi.org/10.1016/j.jallcom.2010.01.002.

[19] Z. Shi, K.M. Liang, S.R. Gu, Effects of CeO2 on phase transformation towards cordierite in 2MgO–Al2O3 –SiO2 system,

Mater. Lett. 51 (2001) 68–72. https://doi.org/10.1016/S0167-577X(01)00267-1.

[20] A.W.A. El-Shennawi, M.M. Morsi, S.A.M. Abdel-Hameed, Effect of fluoride nucleating catalysts on crystallization of cordierite from modified basalt-based glasses, J. Eur. Ceram. Soc. 27 (2007) 1829–1835. https://doi.org/10.1016/j.jeurceramsoc.2006.05.062.

[21] G.-h. Chen, Sintering, crystallization, and properties of CaO doped cordierite-based glass–ceramics, J. Alloys Compd. 455 (2008) 298–302. https://doi.org/10.1016/j.jallcom.2007.01.036.

[22] Y. Yu, X. Hao, L. Song, Z. Li, L. Song, Synthesis and characterization of single phase and low temperature co-fired cordierite glass-ceramics from perlite, J. Non-Cryst. Solids. 448 (2016) 36–42. https://doi.org/10.1016/j.jnoncrysol.2016.06.039.

[23] K. Maeda, Y. Sera, A. Yasumori, Effect of molybdenum and titanium oxides on mechanical and thermal properties of cordierite–enstatite glass-ceramics, J. Non-Cryst. Solids. 434 (2016) 13–22. https://doi.org/10.1016/j.jnoncrysol.2015.12.001.

[24] J. Kang, J. Wang, X. Zhou, J. Yuan, Y. Hou, et al., Effects of alkali metal oxides on crystallization behavior and acid corrosion resistance of cordierite-based glass-ceramics, J. Non-Cryst. Solids. 481 (2018) 184–190. https://doi.org/10.1016/j.jnoncrysol.2017.10.048.

[25] W. Yu, S. Cao, J. Wang, Z. Zhang, J. Han, et al., Crystallization mechanisms of cordierite glass-ceramics with "surface-center" crystallization behavior, J. Eur. Ceram. Soc. 41 (2021) 6708–6721. https://doi.org/10.1016/j.jeurceramsoc.2021.05.061.

[26] X. Lao, X. Xu, Crystallization behavior and properties of non-stoichimetric cordierite glass–ceramics: Effects of talc, MgO/SiO2 ratio, and Al2O3 content, Mater. Today Commun. 31 (2022) 103316. https://doi.org/10.1016/j.mtcomm.2022.103316.

[27] H. Malekzadeh, M. Rezvani, B. Shaabani, Crystallization and sintering behavior of Sol-Gel derived cordierite glass-ceramic containing CaO and B2O3 additives, J. Adv. Mater. Process. 8 (2014) 39–50.

[28] G. H. Chen, Effect of replacement of MgO by CaO on sintering, crystallization and properties of MgO-Al2O3-SiO2 system glass-ceramics, J. Mater. Sci. 42 (2007) 7239–7244. https://doi.org/10.1007/s10853-007-1548-3.

[29] J.-M. Wu, S.-P. Hwang, Effects of (B2O3, P2O5) additives on microstructural development and phase-transformation kinetics of stoichiometric cordierite glasses, J. Am. Ceram. Soc. 83 (2000) 1259–1265. https://doi.org/10.1111/j.1151-2916.2000.tb01364.x.

[30] S. Wang, F. Kuang, Sol-gel preparation and infrared radiation property of boron-substituted cordierite glass-ceramics, J. Mater. Sci.

Technol. 26 (2010) 445–448. https://doi.org/10.1016/S1005-0302(10)60070-9.

[31] C.-F. Yang, C.-M. Cheng, The influence of B2O3 on the sintering of MgO-CaO-Al2O3-SiO2 composite glass powder, Ceram. Int. 25 (1999) 383–387. https://doi.org/10.1016/S0272-8842(98)00049-2.

[32] S.M. Ohlberg, D.W. Strickler, Determination of percent crystallinity of partly devitrified glass by X-ray diffraction, J. Am. Ceram. Soc. 45 (1962) 170–172. https://doi.org/10.1111/j.1151-2916.1962.tb11114.x.

[33] M.S. Shakeri, M. Rezvani, Optical properties and structural evaluation of Li2O–Al2O3–SiO2–TiO2 Glassy semiconductor containing passive agent CeO2, Spectrochim. Acta A: Mol. Biomol. Spectrosc. 83 (2011) 592–597. https://doi.org/10.1016/j.saa.2011.09.009.

[34] M. Sales, G. Alarcon, Crystallization of sol-gel derived glass-ceramic powders in the CaO-MgO-Al2O3-SiO2 system, part II, J. Mater. Sci. 30 (1995) 2341–2347. https://doi.org/10.1007/BF01184584.

[35] R. Petrović, D. Janacković, S. Zec, S. Drmanić, L. Kostić-Gvozdenović, Phase-transformation kinetics in triphasic cordierite gel, J. Mater. Res. 16 (2001) 451–458. https://doi.org/10.1557/JMR.2001.0068.

[36] D. Pal, A.K. Chakraborty, S. Sen, S.K. Sen, The synthesis, characterization and sintering of sol-gel drived cordierite ceramics for electronic applications, J. Mater. Sci. 31 (1996) 3995–4005. https://doi.org/10.1007/BF00352661.

[37] M. Reben, H. Li, Thermal stability and crystallization kinetics of MgO–Al2O3–B2O3–SiO2 glasses, Int. J. Appl. Glass Sci. 2 (2011) 96–107. https://doi.org/10.1111/j.2041-1294.2011.00039.x.

[38] U. Grob, S. Rudiger, E. Kemnitz, Alkaline earth fluorides and their complexes: A sol- gel flourination study, Solid State Sci. 9 (2007) 838–842. https://doi.org/10.1016/j.solidstatesciences.2007.06.008.

[39] M.R. Majhi, R. Pyari, S.P. Singh, Studies on preparation and characterizations of CaO- Na2O- SiO2- P2O5 bioglass ceramics substitued with Li2O, K2O, ZnO, MgO and B2O3, Int. J. Sci. Eng. Res. 2 (2011) 5509–5518.

[40] D.P. Mukherjee, S.K. Das, Effect of nano silica on synthesis and properties of glass-ceramics in SiO2- Al2O3- CaO- CaF2 glass system: A Comparison, J. Non-Cryst. Solids. 368 (2013) 98–104. https://doi.org/10.1016/j.jnoncrysol.2013.03.012.

[41] B. Karmakar, M. Das, S.P. Singh, K. Pal, S. Jena, Influence of combined Al2O3-SiO2 filler on thermal and dielectric properties of barium zinc borate glass Micro-composites for barrier ribs of plasma display panels, Indian J. Eng. Mater. Sci. 17 (2010) 199–207. https://doi.org/10.1080/0371750X.2010.11090821.